Journal of Scientific & Industrial Research
Vol. 83, July 2024, pp. 711-720
DOI: 10.56042/jsir.v83i7.874

Ultrasound Assisted Synthesis of Fe Doped TiO_2 Nanoparticles for Enhanced Photocatalytic Degradation of Ciprofloxacin

Dipak Giram, Tanvi Shrivastava & Arijit Das*

Department of Chemical Engineering, Visvesvaraya National Institute of Technology, Nagpur 440 010, Maharashtra, India

Received 25 April 2023; revised 18 April 2024; accepted 13 June 2024

The present study focused on the photo catalytic degradation of Ciprofloxacin (CP) using ultrasonically synthesized TiO_2 and Fe-doped TiO_2 (1 wt%) nanoparticles under sunlight. The synthesized nanoparticles were extensively characterized using XRD, FTIR, FESEM and EDS techniques. XRD analysis revealed that Fe^{+3} ions were successfully incorporated into TiO_2, and both TiO_2 and Fe-doped TiO_2 nanoparticles contained only anatase phase. The average crystallite size of synthesized nanoparticles was estimated to be in the range of 4-6 nm. The EDS analysis has confirmed the existence of Fe in the sample of Fe-doped TiO_2. The CP degradation study was performed and compared using synthesized nanoparticles. The optimized value of the degradation was investigated by varying experimental parameters, namely, irradiation time, catalyst dosage, initial CP concentration, and pH. Fe-doped TiO_2 nanoparticles outperformed compared to pure TiO_2 nanoparticles for CP degradation. The maximum CP degradation was achieved around 87% at a catalyst dosage of 30 mg, initial CP concentration of 10 ppm, pH of 5, and irradiation time of 150 minutes.

Keywords: Anatase phase, Ultrasonically synthesized, Photocatalysis, Nanocomposite, Wastewater treatment

Introduction

The pharmaceutical industry has evolved significantly throughout the world. Since the last few decades, the faster rate of population growth, outburst of infectious diseases, and the extensive use of antibiotics have widened the growth of the pharmaceutical industry. However, the extensive use of antibiotics and their discharge into the environment from municipal, household, hospitals and pharmaceutical industry cause a potential threat to the health of humans, animals and aquatic life.[1,2]

Ciprofloxacin (CP, $C_{17}H_{18}FN_3O_3$) is a commonly used antibiotic for treating respiratory and urinary infections.[3,4] Nevertheless, it has been identified as a significant aquatic pollutant due to its occurrence in the environment. The persistence of CP in the environment may pose a risk to both the ecosystem and human health, and its resistance to biodegradation makes it difficult to eliminate.[5] The discharge of untreated antibiotics into water bodies can lead to the accumulation of antibiotic-resistant bacteria.[6] Hence, the degradation of CP antibiotic to its harm less form is a most desirable step before discharging to environment.

In recent years, several conventional techniques including coagulation, electrocoagulation, adsorption, and activated sludge process were used for the degradation of antibiotics like CP from wastewater. However, these methods have been found to exhibit certain drawbacks.[7] As a result, an effective treatment method is required to address this issue. Advanced Oxidation Processes (AOPs) are excellent treatment methods for antibiotic degradation. The mechanism of AOPs is to produce reactive species, such as the hydroxyl radical ($OH^{\bullet}$), that can rapidly and non selectively oxidize organic molecules.[8] Among AOPs, photocatalysis technology has been widely used to degrade antibiotics due to its advantages which include high separation efficiency, cheap cost, safety, and the potential to utilize sunlight as their primary energy source. Photocatalysis involves the use of a semiconductor material, such as ZnO, TiO_2, Fe_2O_3, CdS, SnO_2, ZnS, CeO_2, and WO_3 as photocatalyst.[9–11]

Among various photocatalysts, Titanium dioxide (TiO_2) is a widely utilized photocatalyst because of its high stability, low cost, and non-toxicity.[12] Despite the remarkable properties of TiO_2 photocatalyst, some limitations need to be addressed. One of the major limitations is the wide bandgap (3.2 eV) of TiO_2, which restricts its absorption of visible light. This limits the photocatalytic activity of TiO_2 to the UV region only. Additionally, another limitation of TiO_2 photocatalyst is its high electron-hole pair recombination rate, which decreases its

*Author for Correspondence
E-mail: arijitdas@che.vnit.ac.in

performance.[13] To overcome these limitations, various strategies have been explored, including doping with transition metal ions such as iron (Fe).[14,15] It has been reported that Fe-doped TiO_2 can increase the photocatalytic activity of TiO_2 by lowering the electron-hole recombination rate and enhancing the lifespan of charge carriers.[16,17]

The preparation of Fe-TiO_2 nanomaterials is commonly achieved through various synthesis methods including sol-gel method[18], co-precipitation method[19,20], solvo thermal method, molten salt method[21] and hydrothermal method.[22] However, these conventional methods suffer from various limitations such as low yield, utilization of hazardous and costly chemicals, and the requirement for specialized equipment. Furthermore, these methods are time consuming due to requirement of multiple steps and precise control.[17] Hence, there is a need for the development of a novel, uncomplicated, efficient, and cost-effective approach. The ultrasound assisted synthesis method emerged as a promising strategy for producing nanomaterials photocatalysts. During ultrasound assisted synthesis, ultrasound waves generate acoustic cavitation, which causes the formation of localized high-pressure zones (1000 bar) and high temperatures (around 5000 K), leading to the formation of nanoparticles. The energy released during cavitation intensifies micro-mixing, thereby enhancing mass transfer, including solute transfer rate and nucleation rate. The fragmentation of particles into smaller sizes is primarily attributed to the formation and collapse of cavitation bubbles, which generate microjets that break down the particles. Also, this method provides several advantages such as uniform particle size distribution, high purity and high surface area which are essential for efficient photocatalytic activity.[23–26]

In this context, Fe doped TiO_2 (Fe/TiO_2) nanoparticles were prepared through an ultrasound-assisted method. The main objective of this research paper is to investigate the photocatalytic degradation of ciprofloxacin (CP) antibiotic using Fe doped TiO_2 (Fe/TiO_2) nanoparticles synthesized. The present study aims to fill the existing gap in the literature by exploring the photocatalytic activity of Fe/TiO_2 nanoparticles in the degradation of CP antibiotic under sunlight. Additionally, this research focused on optimizing photocatalytic variables such as irradiation time, catalyst dosage, initial pH, and CP concentration using a one-parameter-at-a-time approach to enhance the efficiency of the degradation process.

Materials and Methods

Materials

Iron nitrate nonhydrate ($Fe(NO)_3$ $9H_2O$,purity 97%), sodium hydroxide (NaOH,purity 98%), isopropanol (C_3H_8O, purity 99.5%), Titanium (IV) isopropoxide ($C_{12}H_{28}O_4Ti$, purity 97%) were obtained from M/s Merck India. CP antibiotic was purchased from the medical store, Nagpur. Analytical-grade chemicals were directly used for synthesis of nanoparticles.

Ultrasound-assisted Synthesis of Fe/TiO_2 Nanoparticles

Initially, 5 mL titanium (IV) isopropoxide and measured amount of iron nitrate (0.0135 g) were mixed with 50 mL of isopropanol to prepare a solution-A. The mixture was then subjected to ultrasonication (Dakshin probe sonicator, 180 W, 22 kHz, 4 sec on, 5 sec off) for 15 minutes at room temperature (25–30°C). Afterwards, 50 mL of sodium hydroxide solution-B(1.327 M) was added slowly to the solution-A, followed by an additional 20 minutes of sonication. Following sonication, the reaction mass was filtered and dried at 100°C for 2 hours to get Fe/TiO_2 (1 wt%) nanoparticles powder. A schematic representation of the synthesis process for Fe-doped TiO_2 is depicted in Fig. 1. Pure TiO_2 was synthesized in similar way without addition of ferric nitrate in above process.

Characterization of Fe/TiO_2 Nanoparticles

The crystal structure of synthesized nanoparticles was analyzed utilizing Rigaku Mini-Flex X-ray Diffractometer. The FTIR spectra of synthesized nanoparticles were obtained using a Shimadzu IR-Affinity spectrophotometer. A FESEM (Carl Zeiss, Germany) equipped with an EDS spectrophotometer was used to examine the nanoparticles surface shape and elemental composition. A LABINDIA UV-3200 spectrophotometer was employed to record UV-Visible spectra of samples.

Photocatalytic Degradation of CP

The synthesized nanoparticles were utilized to monitor the photocatalytic activity by degrading an aqueous solution of CP antibiotic under sunlight. To conduct the batch experiment, required amount of Fe/TiO_2 nanoparticles were introduced to 100 mL of CP solution with a composition of desired ppm. The

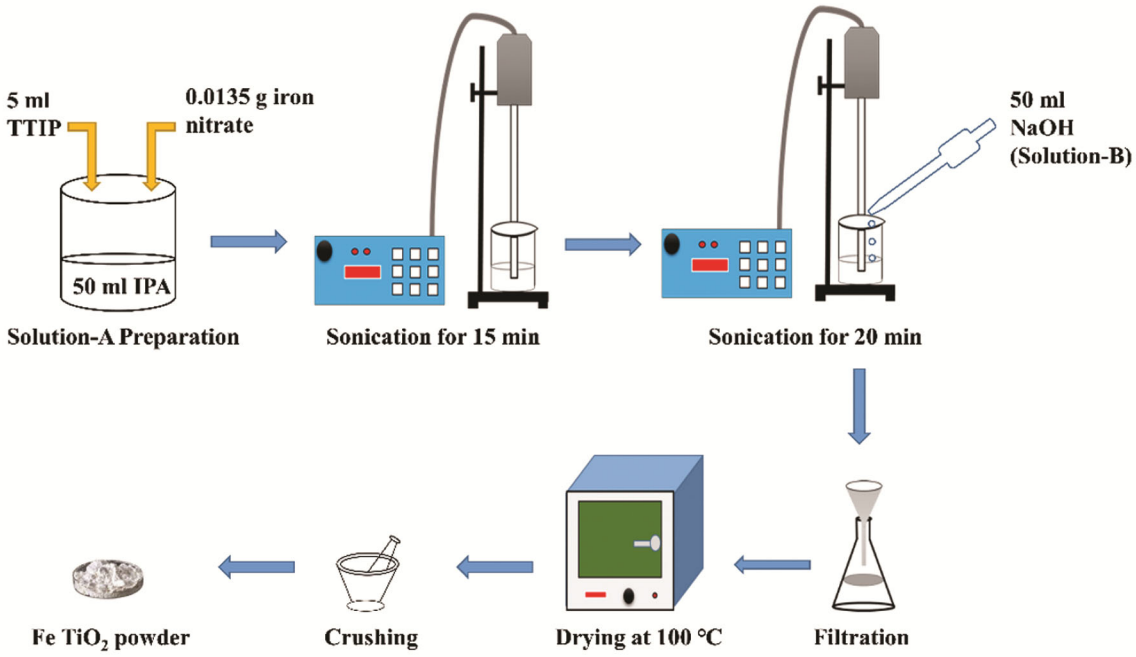

Fig. 1 — Schematic representation of Fe-doped TiO_2 nanoparticles synthesis

resulting mixture was stirred vigorously in darkness for 30 minutes to establish adsorption-desorption equilibrium. The 3 mL samples were collected from the reaction mixture, centrifuged (4000 RPM), and the absorbance of centrifugate was measured (λ_{max} = 276 nm) utilizing a UV-Visible spectrophotometer to determine the concentration of CP. The percentage of CP degradation was determined using the following equation[27]

$$\% \text{ degrdation} = \left(1 - \frac{C}{C_0}\right) \times 100 \quad \ldots (1)$$

where, C_0 and C represents initial and final concentration of CP respectively.

The degradation of CP using synthesized photocatalyst were investigated with respect to various experimental factors, including the type of catalyst (doped TiO_2 and undoped TiO_2), catalyst concentration (10, 30, 50 and 100 mg), initial concentration of CP (10, 20, 30, 50 and 100 ppm), pH values (2, 5, 7, 9 and 12) and irradiation time ranges (0–240 minutes).

Result and Discussion

XRD and FTIR

The XRD of the synthesized TiO_2 and Fe/TiO_2 nanoparticles are shown in Fig. 2(a). The peaks at 2θ = 25.32°, 38.1°, 48.1°, 54.4°, 62.9°,69.8°, and 75.2° correspond to the (101), (112), (200), (105), (204), (220) and (215) planes of anatase TiO_2 respectively (JCPDS No. 21-1272).[28,29] No peaks corresponding to the rutile phase were detected. These results confirm that both TiO_2 and Fe/TiO_2 nanoparticles exhibited anatase phase only. The key diffraction peaks observed in both doped and undoped TiO_2 particles appear to be the same. It suggests that the quantity of Fe dopant was extremely low. However, a small deviation in the peak position from 25.32° to 25.2° was observed in the (101) plane TiO_2 and Fe/TiO_2 nanoparticles, indicating the incorporation of Fe in TiO_2 nanoparticles. Further, The average crystallite size of synthesized nanoparticles was determined using the Debye- Scherrer formula.[28] The average nano-crystallite size of both nanoparticles was calculated in the range of 4–6 nm. The Fe-TiO_2 nanoparticles exhibited smaller crystallite sizes compared to pure TiO_2 nanoparticles, indicating a hindering effect of Fe on TiO_2 crystallization, as reported in previous studies.[29] The substitution of Ti^{4+} ions with Fe^{3+} ions causes distortion of the TiO_6 octahedra, resulting in a strong charge difference and oxygen deficiency in the structure. This phenomenon generates large dipole moments and internal polarization fields in the structure which increases the photocatalytic performance of Fe/TiO_2 sample.[29]

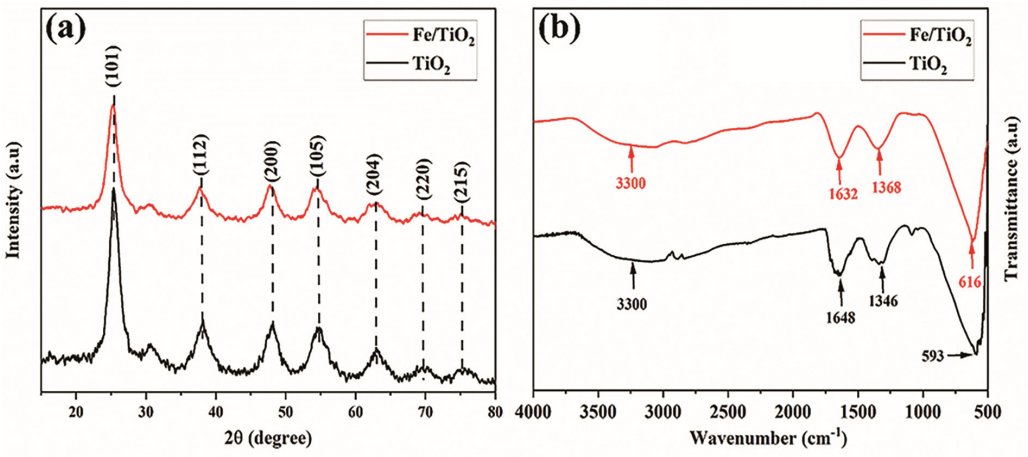

Fig. 2 — (a) XRD patternof TiO_2 and Fe/TiO_2 photocatalyst, (b) FTIR of TiO_2 and Fe/TiO_2 photocatalyst

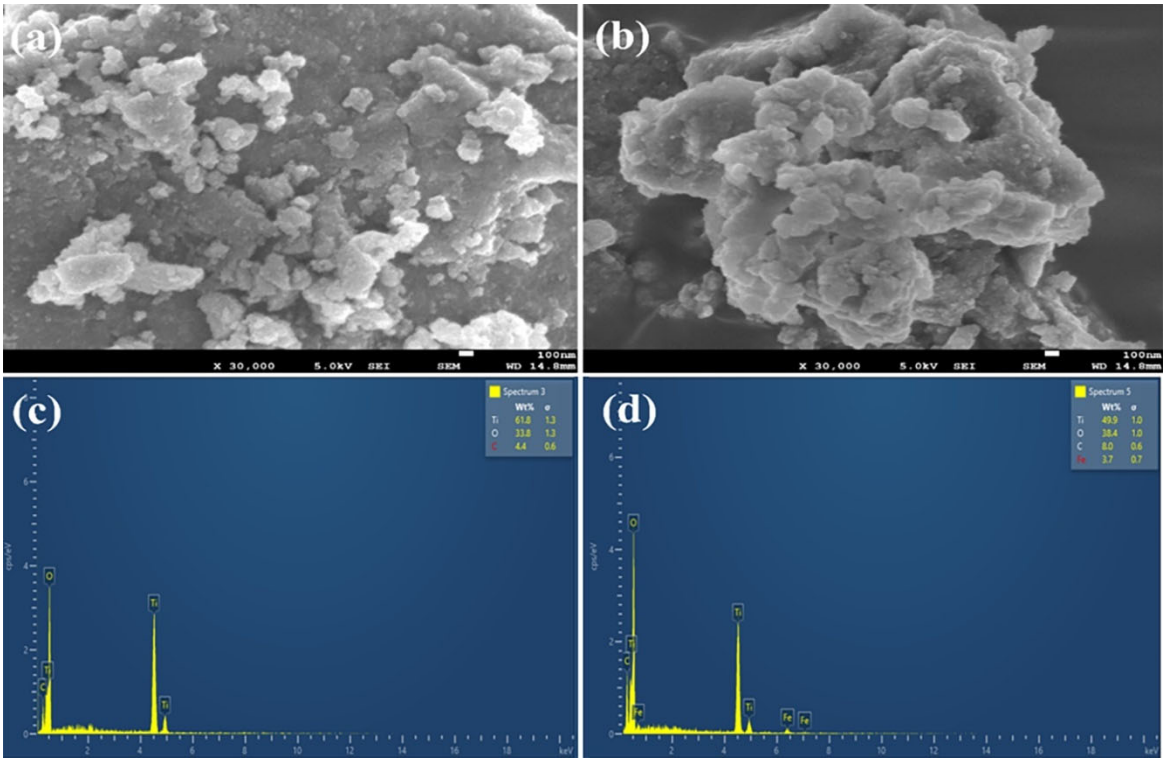

Fig. 3 — (a, c) FESEM and EDS analysis of TiO_2, (b, d)FESEM and EDS analysis of Fe/TiO_2 photocatalysts

The FTIR spectrum of the synthesized nanoparticles is depicted in Fig. 2(b). The broad low intensity peak at 3300 cm^{-1} and 1632 cm^{-1} is due to surface hydroxyl group O-H stretching vibration and surface-adsorbed water molecule bending vibration, respectively.[30] The appearance of hydroxyl group (OH) enhances the photocatalytic activity of synthesized nanoparticles in sunlight. The absorption band near 1368 cm^{-1} is responsible for the symmetric stretching of (C = O).[31] The stretching vibrations of Ti-O and the Ti-O-Ti bond are responsible for the broad peaks observed in the range of 500 to 650 cm^{-1}. The lack of any peak within the wave number range of 1050 to 1200 cm^{-1} indicates that doping was done in the TiO_2 lattice.[32]

FESEM and EDS

FESEM was conducted to study surface morphology of nanoparticles. The images obtained from the FESEM analysis are shown in Fig. 3(a & b). The images (a & b) revealed that the Fe/TiO_2 powders were composed of primary particles that were nano-sized and agglomerated into larger

Table 1 — EDS analysis of each sample with corresponding weight percentages

Elements	TiO_2 (wt%)	Fe/TiO_2 (wt%)
Zn	61.8	49.9
O	33.8	38.4
Fe	—	3.7
C	4.4	8
Total	100	100

powder particles. In contrast, pure TiO_2 consisted of smaller agglomerated nanoparticles. This suggests that the doping of Fe into the TiO_2 increased the degree of agglomeration, as reported by Moradi *et al*.[28]

The EDS spectra obtained from the analysis is depicted in Fig. 3(c & d). The results demonstrated that the synthesized nanoparticles included titanium, iron, carbon and oxygen elements. The presence of iron (Fe) confirms the successful doping of TiO_2 nanoparticles with Fe. The weight percentage of Ti, Fe, and O was found to be 49.9%, 3.7%, and 38.4%, respectively. The detection of carbon in the EDS spectra suggests its presence in the nanoparticles, possibly originating from carbon-containing precursors used during synthesis or residual carbon from precursor materials. Furthermore, carbon-based surface modifications applied during sample coating for EDS analysis could also contribute to the carbon signal observed in the EDS spectrum. The detailed weight percentages of each synthesized sample are depicted in Table 1.

Photocatalytic Activity of CP Degradation

Effect of Irradiation Time

To examine the impact of irradiation time on CP degradation, a 100 mL solution of 20 ppm CP (pH = 5) was subjected to various irradiation times (0 to 240 min) in the presence of 10 mg of the synthesized photocatalyst. The resulting degradation of CP was measured and plotted in Fig. 4(a). The experimental findings showed co-relation between irradiation time and degradation percentage. The optimal reaction time for achieving the highest removal efficiency was found to be 150 minutes, which allowed for the effective generation of hydroxyl radicals ($OH^{\bullet}$) and their subsequent reaction with target chemicals.[33] However, the degradation rate remained constant or decreased after 150 minutes, which can be attributed to the generation of other byproducts that are more challenging to remove or treat.

Effect of Adsorption, Photolysis, Photocatalysis Process

The present study investigates the degradation of CP using three different processes, namely adsorption (in the absence of light but with a catalyst), photolysis (in the presence of light but without a catalyst), and photocatalysis (in the presence of both light and a catalyst). The batch experiments were conducted using an initial CP concentration of 20 ppm, a pH of 5, a catalyst loading of 10 mg, and maximum irradiation of 150 minutes. The results are depicted in Fig. 4(b). After 150 minutes of photolysis, no degradation of CP occurred, indicating that photolysis alone is an inefficient method for CP degradation under sunlight.[34] However, the adsorption of CP molecules onto TiO_2 and Fe/TiO_2 resulted in the removal of 11.12% and 21.27% of CP, respectively. However, in the photocatalysis process, TiO_2 (61.34%), and Fe/TiO_2 (76.93%) exhibited true degradation compared to adsorption due to the production of hydroxyl radicals, which act as oxidizing agents. The results revealed that the photocatalysis of CP with Fe/TiO_2 was effective than pure TiO_2 due to the reduction in the band gap. However, the photocatalytic degradation of pure TiO_2 under sunlight illumination is low due to the larger band gap (3.2 eV), which results in lower absorption of visible light. Therefore, Fe/TiO_2 produced the best outcomes, making it the preferred choice for further experiment.

Effect of Catalyst Loading

One of the key criteria affecting the performance of the photocatalytic process is the amount of catalyst loading. The impact of catalyst dosage of Fe/TiO_2 photocatalyst is depicted in Fig. 4(c). This investigation maintained constant values of other parameters, including an initial concentration of CP at 20 ppm, pH at 5, and irradiation time of 150 minutes. The amounts of catalyst 10, 20, 30, 40, 50 and 100 mg were used which corresponds to the overall degradation of 75.54, 79.53, 83.44, 80.47, 73.09 and 47.21%, respectively. The photocatalytic degradation of CP using Fe/TiO_2 nanoparticles showed that the degradation efficiency increased with increasing catalyst loading up to 30 mg, beyond which the degradation efficiency remained constant. The maximum degradation efficiency of 83.44% was obtained at a catalyst dosage of 30 mg. The higher degradation efficiency at higher catalyst dosage is due to the availability of more active sites for the reaction. However, at higher catalyst loadings, the formation of

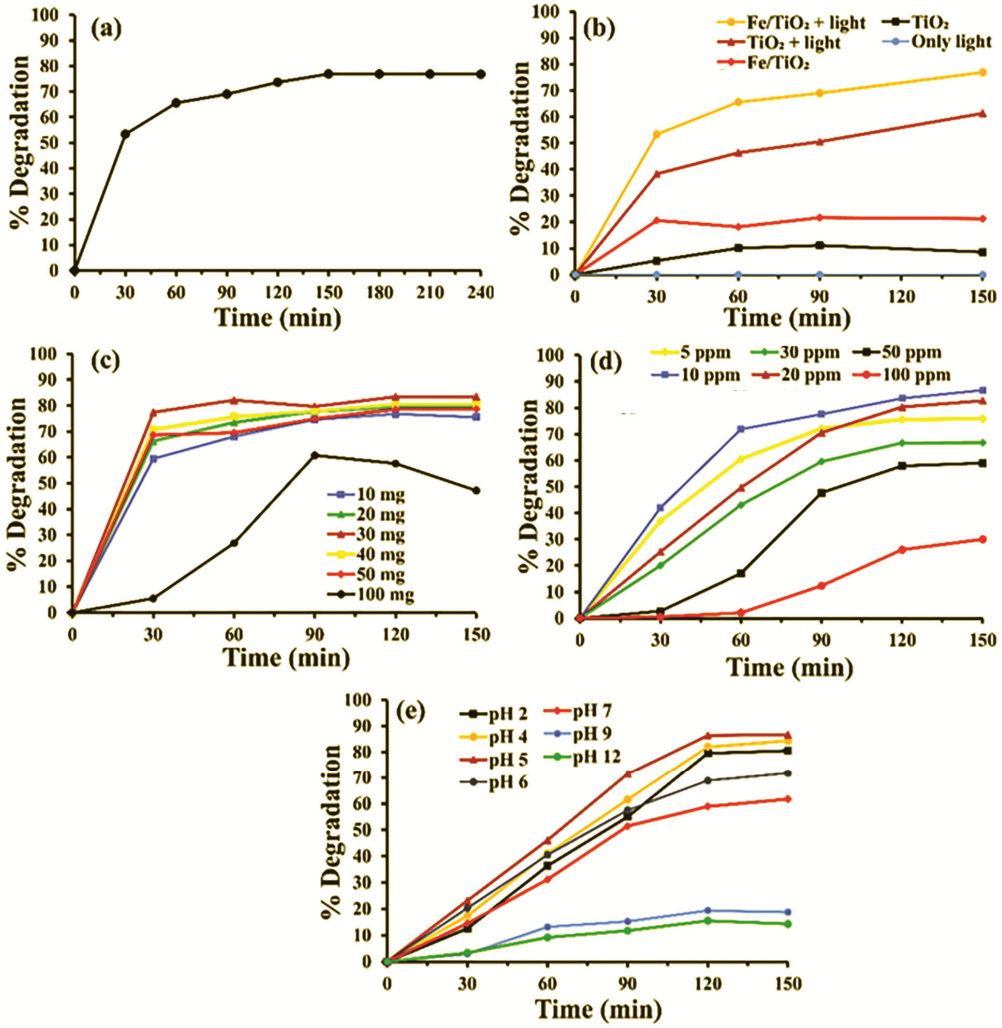

Fig. 4 — Effect of various parameters on CP degradation using Fe/TiO_2 photocatalyst(a) irradiation time [conditions: catalyst loading = 10 mg, initial CP concentration = 20 ppm, pH = 5], (b) different processestime [conditions: catalyst loading = 10 mg, initial CP concentration = 20 ppm, pH = 5, time = 150 min], (c) catalyst loading [conditions: initial CP concentration = 20 ppm, pH = 5, time =150 min], (d) initial CP concentration [conditions: catalyst loading = 30 mg, pH = 5 , time = 150 min], and (e) pHof CP [conditions: catalyst loading = 30 mg, initial CP concentration = 10 ppm, time = 150 min]

aggregates could limit the diffusion of CP to the active sites, resulting in a constant or less degradation efficiency.[27]

Effect of Initial Concentration of CP

The experimental results depicted in Fig. 4(d) investigate the impact of varying initial concentrations of CP (ranging from 5 to 100 PPM) on its degradation rate when subjected to a fixed optimal photocatalyst dosage of 30 mg and maintained at a constant pH 5. The degradation of CP increased with an increase in concentration from 5 ppm to 10 ppm. However, further increases in concentration beyond 10 ppm resulted in a decrease in CP degradation. Specifically, after a total irradiation time of 150 minutes, the degradation percentage for the 10 ppm CP was determined to be 86.76%, whereas for the 100 ppm concentration, it dropped to 30.03%. This is due to the fact that at lower initial concentrations of CP, the degradation kinetics are fast as the availability of higher number of reactive sites on the Fe/TiO_2 nanoparticles. However, at higher initial concentrations of CP, the reaction rate is slower due to the saturation of the reactive sites by intermediates of CP on the Fe/TiO_2 nanoparticles. Also, the solution with high concentration prevents the transmission of light on to the surface of the photocatalyst, leading to less utilization of light.[35] Therefore, the initial concentration of CP needs to be carefully considered to optimize the degradation efficiency.

Effect of pH

The pH of the solution can significantly influence the adsorption of CP molecules on the catalyst surface. After determining the optimal conditions in previous steps, the impact of varying pH levels (2,4,5,6, 7, and 9,12) on the degradation of CP is illustrated in Fig. 4(e), while holding other parameters (catalyst loading 30 mg and initial CP concentration 10 ppm) constant. The results were consistent with the fact that the photodegradation efficiency exhibits a gradual increase with the pH value rising from 2 to 5. However, a gradual decrease in the photodegradation efficiency was observed with a rise in pH value from 7 to 12. According to the point of zero charge (PZC) analysis, the pH_{pzc} of TiO_2 nanoparticles is in the range of 5.6 to 6.4.[36] It was observed that The Fe/TiO_2 nanoparticles surface exhibits a negative charge at pH values above pH_{pzc} and a positive charge at pH values below pH_{pzc}. As the pH value approaches to the pH_{pzc} of Fe/TiO_2 nanoparticles, neutral CP molecules tend to be readily transferred and concentrated onto the surface of the Fe/TiO_2 photocatalyst surface. This phenomenon ultimately leads to increased degradation of CP. Furthermore, under basic conditions (at high pH values) both photocatalyst and CP showed negative charges, resulting in electrostatic repulsion between them, which led to a decreased photodegradation of CP.[34,37]

Effect of Doping at Optimized Conditions

In this study, the degradation of CP solution was investigated for 150 minutes. This study was conducted using optimized loading of TiO_2 and Fe/TiO_2 photocatalysts, with a catalyst loading of 30 mg, initial CP concentration of 10 ppm, and pH of 5. The results indicated that the Fe/TiO_2 nanocomposite exhibited a higher degradation efficiency of 86.78% compared to pure TiO_2 at 65.85% under the same conditions (as shown in Fig. 5(a). The improved photocatalytic performance of the Fe/TiO_2 photocatalyst was due to its effective charge separation, leading to a significant reduction in electron and hole pairs recombination rate. Additionally, the time-dependent degradation of CP using Fe/TiO_2 photocatalyst under optimized conditions is demonstrated (Fig. 5b) in the UV-visible absorption spectra. The degradation process was monitoredby analyzing the changes in the absorbance spectrum of the CP before and after treatment. The result exhibit that CP has a characteristic absorption peak at a 276 nm (λ_{max}) wavelength in their UV-Vis spectrum before degradation (time = 0 min). However, after 150 minutes time, the characteristic absorption peak at 276 nm disappeared, signifying the successful degradation of CP.

In summary, the results of the degradation measurements for CP indicate that Fe/TiO_2 nanoparticles is highly effective photocatalyst. The performance of the Fe/TiO_2 nanoparticles for degrading ciprofloxacin is presented in Table 2.

Mechanism

The degradation mechanism of the CP antibiotic using Fe/TiO_2 photocatalyst is depicted in Fig. 6. When Fe/TiO_2 is exposed to sunlight, Fe/TiO_2 photocatalyst is stimulated and produces electrons and

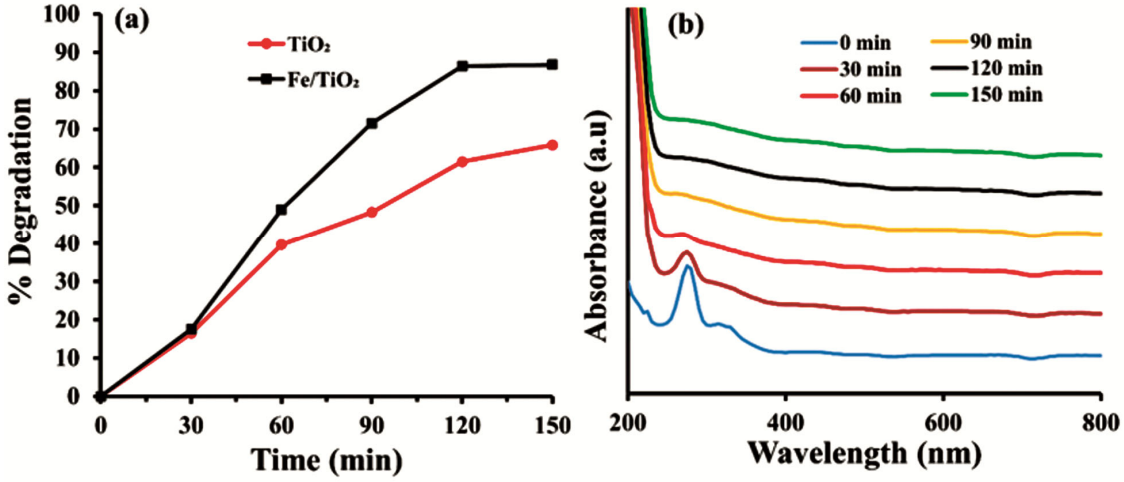

Fig. 5 — (a) Effect of Fe doping on the TiO_2 photocatalyst at optimized conditions for CP degradation [conditions: catalyst loading = 30 mg, initial CP concentration = 10 ppm, pH = 5], and (b) time-dependent UV-visible absorption spectra of CP degradation using Fe/TiO_2 photocatalyst under optimized conditions

Table 2 — Summary of photocatalytic activity of Fe/TiO_2 photocatalyst for CP degradation

Photocatalyst	Catalyst loading (mg)	Ciprofloxacin initial concentration (ppm)	pH	Process	Irradiation time (min)	% degradation
		Effect of irradiation time				
Fe/TiO_2	10	20	5	Photocatalysis	**30**	53.37
Fe/TiO_2	10	20	5	Photocatalysis	**60**	65.60
Fe/TiO_2	10	20	5	Photocatalysis	**90**	69.01
Fe/TiO_2	10	20	5	Photocatalysis	**120**	73.68
Fe/TiO_2	10	20	5	Photocatalysis	**150**	76.93
Fe/TiO_2	10	20	5	Photocatalysis	**180**	76.89
Fe/TiO_2	10	20	5	Photocatalysis	**210**	76.87
		Effect of different processes				
No catalyst	10	20	5	**Photolysis**	150	0
TiO_2	10	20	5	**Adsorption**	150	11.12
Fe/TiO_2	10	20	5	**Adsorption**	150	21.27
TiO_2	10	20	5	**Photocatalysis**	150	61.34
Fe/TiO_2	10	20	5	**Photocatalysis**	150	76.93
		Effect of catalyst loading				
Fe/TiO_2	**10**	20	5	Photocatalysis	150	75.54
Fe/TiO_2	**20**	20	5	Photocatalysis	150	79.53
Fe/TiO_2	**30**	20	5	Photocatalysis	150	83.44
Fe/TiO_2	**40**	20	5	Photocatalysis	150	80.47
Fe/TiO_2	**50**	20	5	Photocatalysis	150	73.9
Fe/TiO_2	**100**	20	5	Photocatalysis	150	47.21
		Effect of Concentration				
Fe/TiO_2	30	**5**	5	Photocatalysis	150	75.89
Fe/TiO_2	30	**10**	5	Photocatalysis	150	86.76
Fe/TiO_2	30	**20**	5	Photocatalysis	150	82.72
Fe/TiO_2	30	**30**	5	Photocatalysis	150	66.75
Fe/TiO_2	30	**50**	5	Photocatalysis	150	59.02
Fe/TiO_2	30	**100**	5	Photocatalysis	150	30.03
		Effect of pH				
Fe/TiO_2	30	10	**2**	Photocatalysis	150	80.50
Fe/TiO_2	30	10	**4**	Photocatalysis	150	84.37
Fe/TiO_2	30	10	**5**	Photocatalysis	150	86.72
Fe/TiO_2	30	10	**6**	Photocatalysis	150	71.69
Fe/TiO_2	30	10	**7**	Photocatalysis	150	62.70
Fe/TiO_2	30	10	**9**	Photocatalysis	150	18.81
Fe/TiO_2	30	10	**12**	Photocatalysis	150	14.36
		Effect of doping				
Fe/TiO_2	30	10	5	Photocatalysis	150	86.78
TiO_2	30	10	5	Photocatalysis	150	65.85

Bold values show change in parameter during photocatalytic process

holes. The incorporation of Fe into a TiO_2 matrix results in a decrease in electrons and holes recombination. This is attributed to the photo-reduction process of Fe^{+3}/Fe^{+2} as described by equations (2) and (3), which facilitates the separation of charge carriers and leads to improved charge transfer efficiency. In this phenomenon, the Fe^{+3} ion undergoes a redox reaction by capturing an electron produced by photoexcitation. The resulting Fe^{+2} ion subsequently convert oxygen molecule into reactive superoxide radicals ($O_2^{-\bullet}$) Concurrently, photogenerated holes are captured by Fe^{+3} and generate reactive hydroxyl radicals ($OH^{\bullet}$). These processes have been documented in equations 4–10. Ultimately, the degradation of CP occurs due to the formation of $OH^{\bullet}$, represented in Eq. (11). The CP degradation mechanism on Fe/TiO_2 photocatalyst can be summarized using following equations[30,38]

$$TiO_2 + h\nu \rightarrow TiO_2\ (h^+ + e^-) \quad \ldots (2)$$

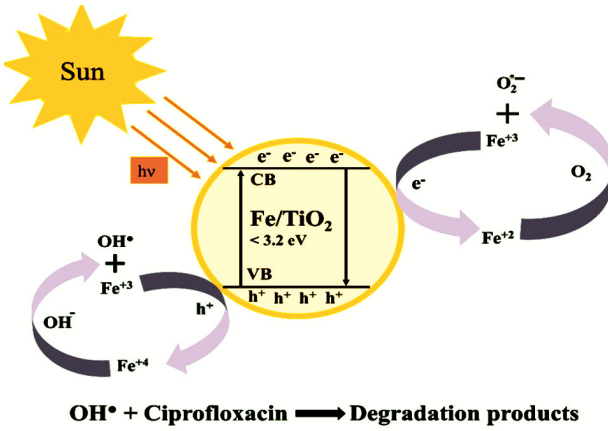

Fig. 6 — Schematic representation of photocatalytic degradation mechanism of CP

$$TiO_2\,(e^-) + Fe^{+3} \rightarrow Fe^{+2} \quad \ldots (3)$$

$$Fe^{+2} + O_2 \rightarrow Fe^{+3} + O_2{}^{-\bullet} \quad \ldots (4)$$

$$Fe^{+2} + Ti^{+4} \rightarrow Fe^{+3} + Ti^{+3} \quad \ldots (5)$$

$$Ti^{+3} + O_2 \rightarrow Ti^{+4} + O_2{}^{-\bullet} \quad \ldots (6)$$

$$O_2{}^{-\bullet} + h^+ \rightarrow O^{-\bullet} \quad \ldots (7)$$

$$O^{-\bullet} + H_2O \rightarrow (OH^{\bullet}) + (OH^-) \quad \ldots (8)$$

$$Fe^{+3} + h^+ \rightarrow Fe^{+4} \quad \ldots (9)$$

$$Fe^{+4} + (OH^-) \rightarrow Fe^{+3} + (OH^{\bullet}) \quad \ldots (10)$$

$$(OH^{\bullet}) + CP\ antibiotic \rightarrow Degradation products \ldots (11)$$

Conclusions

The present study successfully synthesized undoped TiO_2 and Fe-doped TiO_2 nanoparticles using an ultrasound-assisted method and investigated its role for CP degradation. The nanoparticles exhibited the size range of 4–6 nm in its anatase phase. Further, % degradation of CP was optimized by one parameter at a time approach by varying the degradation parameters, irradiation time, catalyst dosage, initial concentration of CP, and pH, respectively. The optimized conditions for highest degradation (86.78%) were achieved at catalyst dosage of 3:10 (w/v), initial CP concentration of 10 ppm, irradiation time of 150 min and pH of 5. This optimization process not only demonstrates the effectiveness of Fe/TiO_2 nanoparticles as a photocatalyst but also provides valuable insights for the design and application of similar systems in wastewater treatment. Furthermore, our findings suggest a promising and environmentally friendly approach for the removal of antibiotics from wastewater.

References

1 Varma K S, Tayade R J, Shah K J, Joshi P A, Shukla A D & Gandhi V G, Photocatalytic degradation of pharmaceutical and pesticide compounds (PPCs) using doped TiO_2 nanomaterials: A review, *Water-Energy Nexus*, **3** (2020) 46–61.

2 Velempini T, Prabakaran E & Pillay K, Recent developments in the use of metal oxides for photocatalytic degradation of pharmaceutical pollutants in water—a review, *Mater Today Chem*, **19** (2021) 100380.

3 Jandaghian F, Ebrahimian Pirbazari A, Tavakoli O, Asasian-Kolur N & Sharifian S, Comparison of the performance of Ag-deposited ZnO and TiO_2 nanoparticles in levofloxacin degradation under UV/visible radiation, *J Hazard Mater Adv*, **9** (2023) 100240.

4 Verinda S B, Muniroh M, Yulianto E, Maharani N, Gunawan G, Amalia N F, Hobley J, Usman A & Nur M, Degradation of ciprofloxacin in aqueous solution using ozone microbubbles:spectroscopic, kinetics, and antibacterial analysis, *Heliyon*, **8(8)** (2022).

5 Hunge Y M, Yadav A A, Kang S W, Jun Lim S & Kim H, Visible light activated MoS_2/ZnO composites for photocatalytic degradation of ciprofloxacin antibiotic and hydrogen production, *J Photochem Photobiol A Chem*, **434** (2023) 114250.

6 Xing X, Du Z, Zhuang J & Wang D, Removal of ciprofloxacin from water by nitrogen doped TiO_2 immobilized on glass spheres: Rapid screening of degradation products, *J Photochem Photobiol A Chem*, **359** (2018) 23–32.

7 Al-Musawi T J, Yilmaz M, Ramírez-Coronel A A, Al-Awsi G R L, Alwaily E R, Asghari A & Balarak D, degradation of amoxicillin under a uv or visible light photocatalytic treatment process using Fe_2O_3/Bentonite/TiO_2: Performance, kinetic, degradation pathway, energy consumption, and toxicology studies, *Optik (Stuttg)*, **272** (2023) 170230.

8 Giram D, Das A & Bhanvase B, Comparative study of ZnO-TiO_2 nanocomposites synthesized by ultrasound and conventional methods for the degradation of methylene blue dye, *Indian J Chem Technol*, **30** (2023) 693–704.

9 Parmar N & Srivastava J K, Process optimization and kinetics study for photocatalytic ciprofloxacin degradation using TiO_2 nanoparticle: A comparative study of artificial neural network and surface response methodology, *J Indian Chem Soc*, **99(8)** (2022) 100584.

10 Kar P, Shukla K, Jain P, Sathiyan G & Kumar R, Nano materials science semiconductor based photocatalysts for detoxification of emerging pharmaceutical pollutants from aquatic systems : A critical review, *Nano Mater Sci*, **3(1)** (2021) 25–46.

11 Giram D & Das A, Synthesis and characterization of Fe doped ZnO nanoparticles for the photocatalytic degradation of eriochrome black-T dy, *Indian J Chem Technol*, **31(1)** (2024) 39–43.

12 Wahyuni E T, Mahira N S, Lestari N D & Natsir T A, Remarkable enhancement of the TiO_2 photocatalyst activity under visible light by doping sulfur for dye photodecolorization, *Indian J Chem Technol*, **29 (5)** (2022) 519–525.

13 Tashkandi N Y, Albukhari S M & Ismail A A, Visible-light driven of heterostructured $LaFeO_3$/TiO_2 photocatalysts for

degradation of antibiotics: Ciprofloxacin as case study, *J Photochem Photobiol A Chem*, **432** (2022) 114078.

14 Anisha R & Vasam E K, Enhanced photocatalytic degradation of azo dye using rare-earth metal doped TiO_2 under visible light irradiation, *Indian J Chem Technol*, **29(5)** (2022) 547–553.

15 Huang W H, Lin C J, Huang T H, Chang C Y, Haw S C, Sheu H S, Chen S Y, Dong C L, Kumar K, Hwang B J, Su W N & Chen C L, Mechanistic study for enhanced photocatalytic degradation of acetaminophen by Fe(III) doped TiO_2 hollow submicrospheres, *Appl Surf Sci*, **611** (2023) 155634.

16 Moradi V, Jun M B, Blackburn A & Herring R A, Significant improvement in visible light photocatalytic activity of Fe doped TiO_2 using an acid treatment process, *Appl Surf Sci*, **427** (2018) 791–799.

17 Valero-Romero M J, Santaclara J G, Oar-Arteta L, Van Koppen L, Osadchii D Y, Gascon J & Kapteijn F, Photocatalytic properties of TiO_2 and Fe-doped TiO_2 prepared by metal organic framework-mediated synthesis, *Chem Eng J*, **360** (2019) 75–88.

18 Ali T, Tripathi P, Azam A, Raza W, Ahmed A S, Ahmed A & Muneer M, Photocatalytic performance of Fe-doped TiO_2 nanoparticles under visible-light irradiation, *Mater Res Express*, **4(1)** (2017) 15022.

19 Ellouzi I, Regraguy B El, Hajjaji S, Harir M, Schmitt-Kopplin P, Lachheb H & Laânab L, Synthesis of Fe-doped TiO_2 with improved photocatalytic properties under visible light irradiation, *Iran J Catal*, **12 (3)** (2022) 283–293.

20 Ismael M, Enhanced photocatalytic hydrogen production and degradation of organic pollutants from Fe (III) doped TiO_2 nanoparticles, *J Environ Chem Eng*, **8(2)** (2020) 103676.

21 Ghorbanpour M & Feizi A, Iron-doped TiO_2 catalysts with photocatalytic activity, *J Water Environ Nanotechnol*, **4(1)** (2019) 60–66.

22 Zhu J, Zheng W, He B, Zhang J & Anpo M, Characterization of Fe–TiO_2 photocatalysts synthesized by hydrothermal method and their photocatalytic reactivity for photodegradation of XRG dye diluted in water, *J Mol Catal A Chem*, **216(1)** (2004) 35–43.

23 Ambati R & Gogate P R, Ultrasound assisted synthesis of iron doped TiO_2 catalyst, *Ultrason Sonochem*, **40** (2018) 91–100.

24 Mahendran V & Gogate P R, Degradation of acid scarlet 3R dye using oxidation strategies involving photocatalysis based on Fe doped TiO_2 photocatalyst, ultrasound and hydrogen peroxide, *Sep Purif Technol*, **274** (2021) 119011.

25 Deshmukh S P, Kale D P, Kar S, Shirsath S R, Bhanvase B A, Saharan V K & Sonawane S H, Ultrasound assisted preparation of rGO/TiO_2 nanocomposite for effective photocatalytic degradation of methylene blue under sunlight, *Nano-Struct Nano-Objects*, **21** (2020) 100407.

26 Bhanvase B A, Veer A, Shirsath S R & Sonawane S H, Ultrasound assisted preparation, characterization and adsorption study of ternary chitosan-ZnO-TiO_2 nanocomposite: Advantage over conventional method, *Ultrason Sonochem*, **52** (2019) 120–130.

27 Manasa M, Chandewar P R & Mahalingam H, Photocatalytic degradation of ciprofloxacin & norfloxacin and disinfection studies under solar light using boron & cerium doped TiO_2 catalysts synthesized by green EDTA-citrate method, *Catal Today*, **375** (2021) 522–536.

28 Moradi H, Eshaghi A, Hosseini S R & Ghani K, Fabrication of Fe-doped TiO_2 nanoparticles and investigation of photocatalytic decolorization of reactive red 198 under visible light irradiation, *Ultrason Sonochem*, **32** (2016) 314–319.

29 Yadav H M, Kolekar T V, Pawar S H & Kim J S, Enhanced photocatalytic inactivation of bacteria on Fe-containing TiO_2 nanoparticles under fluorescent light, *J Mater Sci Mater Med*, **27(3)** (2016) 1–9.

30 Komaraiah D, Radha E, Kalarikkal N, Sivakumar J, Reddy M R & Sayanna R, Structural, optical and photoluminescence studies of sol-gel synthesized pure and iron doped TiO_2 photocatalysts, *Ceram Int*, **45(18)** (2019) 25060–25068.

31 Kayani Z N, Wahid I, Saddiqe Z, Riaz S, Waseem S & Naseem S, Tailoring of optical, biological and magnetic properties of nanocrystalline Fe doped TiO_2 thin films, *Mater Res Express*, **6(12)** (2020) 1250h2.

32 Mishra S, Chakinala N, Chakinala A G & Surolia P K, Photocatalytic degradation of methylene blue using monometallic and bimetallic Bi-Fe doped TiO_2, *Catal Commun*, **171** (2022) 0–4.

33 Nasiri A, Tamaddon F, Mosslemin M H, Gharaghani M A & Asadipour A, New magnetic nanobiocomposite - $CoFe_2O_4$@methycellulose: Facile synthesis, characterization, and photocatalytic degradation of metronidazole, *J Mater Sci Mater Electron*, **30(9)** (2019) 8595–8610.

34 Hassani A, Khataee A & Karaca S, Photocatalytic degradation of ciprofloxacin by synthesized TiO_2 nanoparticles on montmorillonite: Effect of operation parameters and artificial neural network modeling, *J Mol Catal A Chem*, **409** (2015) 149–161.

35 Wen X J, Niu C G, Zhang L, Liang C, Guo H & Zeng G M, Photocatalytic degradation of ciprofloxacin by a novel Z-scheme CeO_2–Ag/AgBr Photocatalyst: influencing factors, possible degradation pathways, and mechanism insight, *J Catal*, **358** (2018) 141–154.

36 Kamani H, Shirazi R H S M, Norabadi E & Hassani A H, Sonocatalytic removal of ciprofloxacin by Fe-doped TiO_2 nanoparticles from aqueous solution, (2021) 1–19.

37 Wang G, Li Y, Dai J & Deng N, Highly Efficient photocatalytic oxidation of antibiotic ciprofloxacin using TiO_2@g-C_3N_4@biochar composite, *Environ Sci Pollut Res*, **29** (2022) 48522–48538.

38 Sood S, Umar A, Mehta S K & Kansal S K, Highly effective Fe-doped TiO_2 nanoparticles Photocatalysts for visible-light driven photocatalytic degradation of toxic organic compounds, *J Colloid Interface Sci*, **450** (2015) 213–223.